air-LUSI: Autonomous telescope design for lunar spectral irradiance measurements

Andrew Cataford[a], S. Andrew Gadsden*[a], and Kevin Turpie[b]

[a]University of Guelph, Guelph, Ontario, Canada, N1G 2W1
[b]University of Maryland, Baltimore County, Baltimore, Maryland, USA, 21075

ABSTRACT

air-LUSI is a NASA sponsored project which uses optical and robotic equipment to autonomously capture radiometric measurements of the Moon from within the science pod of an ER-2 aircraft while flying at an altitude of 70,000 feet. The air-LUSI instrument was deployed for its first engineering flight campaign on August 1st and 2nd, 2018 and captured the worlds first High Altitude Lunar Spectral Irradiance (LUSI) measurements from a semi-ground based system. By implementing instrumentation into NASA's ER-2 aircraft to produce an Airborne Lunar Observatory, unprecedented LUSI measurements can be obtained that are unadulterated from the Earth's atmosphere. By compiling a comprehensive LUSI dataset for a series of lunar phases, a Lunar Calibration Model can be further refined to provide enhanced remote sensing capabilities for some instruments in NASA's Earth Observing System (EOS). This document presents information about the flight path of the ER-2 to capture High Altitude LUSI measurements, the mechanical design of the robotic telescope, the environmental operating conditions of the design, the in flight tracking performance of the system, and the first raw lunar spectrum captured at 70,000 feet.

Keywords: Robotic Telescope, Lunar Spectral Irradiance (LUSI), Control, Machine Vision

1. INTRODUCTION

A partnership between the National Aeronautics and Space Administration (NASA) and the United States Geological Survey (USGS) has been developing a Lunar Calibration model for select instruments of NASA's Earth Observing System (EOS).[1–4] The Moon provides a stable reflective surface for sun light that varies with lunar phase and geometry. By compiling a dataset of accurate measurements, a Lunar Calibration model could be used to improve the remote sensing capabilities of certain satellites.[5] Unfortunately, the current Lunar Spectral Irradiance calibration model has uncertainties within (5-10%) and therefore, the Lunar Spectral Irradiance (LUSI) of the Moon needs to be measured with a higher degree of accuracy to achieve a desired absolute uncertainty of 1%.[6]

Until recently, LUSI measurements had only been acquired using ground based measurement techniques. Ground based measurements allow for the radiometric instruments to be regularly calibrated, which contributes to the overall accuracy of the captured spectrums. Unfortunately, the Earth's atmosphere obstructs key lunar wavelengths and prevents consistent LUSI measurements from being obtained. To achieve a high degree of accuracy, a radiometric measurement system needed to be developed that could be regularly calibrated to guarantee the accuracy of measured spectra, and that could travel to high altitudes to mitigate any spectral degradation and obstruction from the Earth's atmosphere.[7]

The requirement for a high altitude radiometric instrument that is capable of returning to Earth for calibration resulted in the creation of the air-LUSI project. The Remote Sensing Group of the National Institute of Standards and Technology (NIST) designed the telescope and radiometric system required to capture the Lunar Spectral Measurements. A small group at the University of Guelph designed and manufactured the robotic system capable of keeping the Moon centred within the Field of View of the telescope while operating from within a moving aircraft.

Advanced Optics for Imaging Applications: UV through LWIR IV, edited by Jay N. Vizgaitis
Peter L. Marasco, Jasbinder S. Sanghera, Proc. of SPIE Vol. 10998, 109980O

2. SUBSYSTEM DESIGN

2.1 Radiometric System

Individuals at NIST designed a custom telescope specifically for the radiometric subsystem of the air-LUSI mission. The system uses a single lens telescope which is 18.5 inches in length and 6.5 inches in diameter to funnel the light of the Moon to an integrating sphere. The captured moonlight is then relayed to a CAS spectrometer for analysis. Given the sensitivity of the CAS spectrometer to environmental conditions, an environmental enclosure was designed to maintain the atmospheric pressure and temperature of the unit.

The design was based on the extreme environmental conditions in which the system would operate and the construction materials were selected for their thermal stability and strength. The telescope was constructed of carbon fibre tubing with concentric steel rings that double as optical baffles and structural points for integrating the telescope to the robotic structure. The telescope included a pressure fitting that served as an inlet for the nitrogen purge system to prevent moisture from accumulating on the inside of the telescope. The system was designed to be robust and provide accurate measurements given that it would be exposed to high points of humidity, a temperature range of ($23°C$ to $-55°C$), and large atmospheric pressure variation while the aircraft travels from ground level to an altitude of 70,000 ft.

2.2 Robotic Design

The robotic telescope used two linear actuators as a robust, affordable, and simplified means of controlling the system. As a whole, the design consisted of a telescope that was supported by trunnions that mounted to a double gimbal. The gimbal provided two degrees of freedom and allowed the telescope's pointing angles to be adjusted in elevation and azimuth.[8–11] The first linear actuator was mounted on the structural frame that supported the system and used a rod end ball joint to attach to the spindle crank. This provided the moment arm that was used to adjust the telescopes pointing angle in the azimuth. The second linear actuator was mounted within the inner gimbal and connected to the telescope's trunnion platform and allowed for its stroke position to adjust the pointing elevation of the telescope.

By using linear actuators, the number of mechanical components were drastically reduced by eliminating the requirement for gearing, additional bearings, and lubrication.[12–14] The linear actuators relied on a servo motor to turn an internal ACME screw which adjusted their stroke position. Each actuator was interfaced to the robotic control computer and allowed for data and position commands to be written to the actuators.[15]

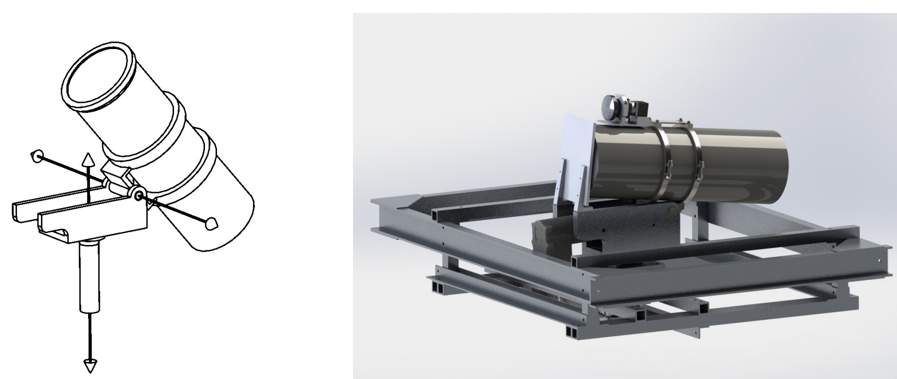

Figure 1. Design concept and rendering of the air-LUSI robotic telescope.

2.3 Mechanical Components

The linear actuators selected for the robotic system were the Ultramotion A2 series servo cylinders. They were specifically selected based on their robust design and their ability to satisfy the harsh environmental conditions encountered during high altitude flights. The linear actuators offered a sealed enclosure with internal humidity control, liquid ingress protection and a temperature range extended to $-45°C$. Thin film heaters and thermostats were attached to the actuators to ensure that their external temperatures did not drop outside of the operating limits.[15,16]

Flight grade self lubricating flanged journal bearings were obtained from Kaman Specialty Bearings and Engineered Products to provide the freedom of rotation required by the design. The Kamatics series journal bearings consisted of a PTFE resin applied to the inside of a stainless steel bushing to offer low friction coefficients for a wide range of temperatures. The PTFE resin is extremely wear resistant, chemically inert, has very low moisture absorption, and can operate in temperatures as low as $-73\,C^{\circ}$. Specifically designed for operating in harsh environments within aerospace applications, the self lubricating bearings provided by Kaman were the obvious choice when selecting bearings for the design.[16–18]

3. CONTROL SYSTEM

3.1 Machine Vision

The Basler Ace U (acA1920-40um) series machine vision camera was the primary data acquisition system used to acquire the Moon as a target and provide tracking information to the control computer. The tracking camera was mounted near the aperture of the telescope and provided an eye in hand vision feedback system used for visual servoing. Once the robotic system was in a tracking mode, the telescope would move up from its stowed position to its initial tracking position which provided the telescope and tracking camera a view of the night sky while operating from within the ER-2 science pod.

The strategy that was used to target the Moon exploited the fact that the missions would be flown at night and that the Moon would be the largest and brightest object in the sky. Given this targeting scenario, the incoming tracking camera frames were thresholded to yield binary images where all the pixels associated with the Moon were white, and all other pixels within the frame were black. Contouring was then performed to locate the boundary of the Moon within the images, and a minimum enclosing rectangle was fit around the target. The center point of the minimum enclosing rectangle was taken as the (x,y) pixel location of the target. This 2D location within the image frame was then passed on as the inputs to the telescope's pointing controllers.[10,11,19–21]

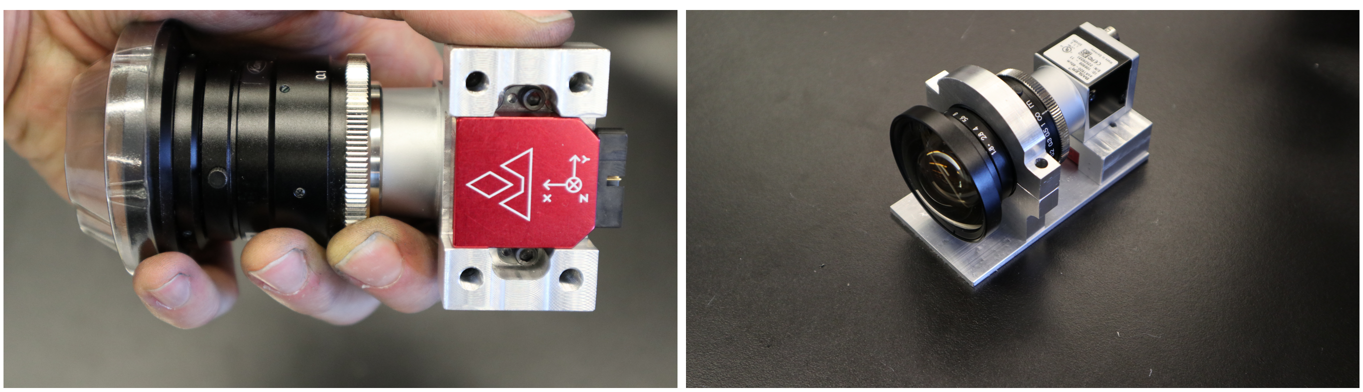

Figure 2. Machine Vision camera and integrated IMU used for data acquisition and target tracking.

3.2 Pointing Controllers

Prior to the flights, the tracking camera and telescope were aligned to determine the pixel position within the tracking camera image that corresponded to a target being centred within the field of view of the telescope. While capturing tracking camera images, the telescope was laser aligned with a distant light source. The location of this light source within the tracking camera image was determined using the same techniques as the targeting system for the Moon. Given that the telescope and tracking camera were viewing the light source from two slightly different vantage points, a parallax correction was made to the y dimensions of the pixel setpoint.[22–26]

The robotic control system used the established pixel setpoint as the desired state of the system and used the target locations within the tracking frame as a state measurement. The difference between the setpoint and the target position in (x,y) within the tracking camera frames provided the two state error measurements that were used as the inputs to the two independent elevation and azimuth PID controllers. Given the magnitude of the state errors in x and y, a control effort was calculated and applied by writing position commands to the linear actuators. The stroke positions of the two linear actuators were then adjusted and forced the pointing error between the telescope and the Moon to converge to zero in azimuth and elevation.[?,27,28]

4. ENGINEERING FLIGHT

The air-LUSI instrument was first deployed on August 1st and 2nd, 2018 for its two night engineering flight campaign. The mission system was tested at the Airborne Sciences Laboratory of NASA Armstrong Flight Research Center (AFRC) and integrated into the right science pod the ER-2 aircraft. The robotic telescope system was located in the aft section of the science pod, which had an upward facing aperture that could be used to view the Moon. The bulk of the radiometric subsystem and the robotic control computer were contained in the somewhat temperature and pressure regulated mid body of the science pod. A bulk head separated the two sections of the science pod and a pass-through plate was fabricated to connect the control computers and measurement equipment to the telescope and the robotic mount.

4.1 Flight Path

A flight path was designed to provide a 40 minute tracking window in which the Moon could be visible to the telescope when looking out from the aft pod aperture. The flight was scheduled in the early hours of the morning and targeted lunar elevations that fell within the line of sight of the design. At approximately (0200) the aircraft took off from AFRC located in Palmdale California, climbed to its maximum altitude traveling in a North Eastern direction, and headed for its initial tracking heading located in the North Western corner of Arizona. At that point, the pilot turned the aircraft to achieve the lunar tracking heading, and maintained the long straight course flying over the southern tip of Nevada. This trajectory provided a forty minute tracking window in which the air-LUSI subsystem was locked onto the Moon collecting valuable spectral measurements. At the end of the tracking phase of the mission, the aircraft abandoned course and quickly returned to AFRC for landing. The entire trajectory is plotted in Figure 3 and was obtained using the navigation data from the ER-2 that was relayed to mission control via ground link.

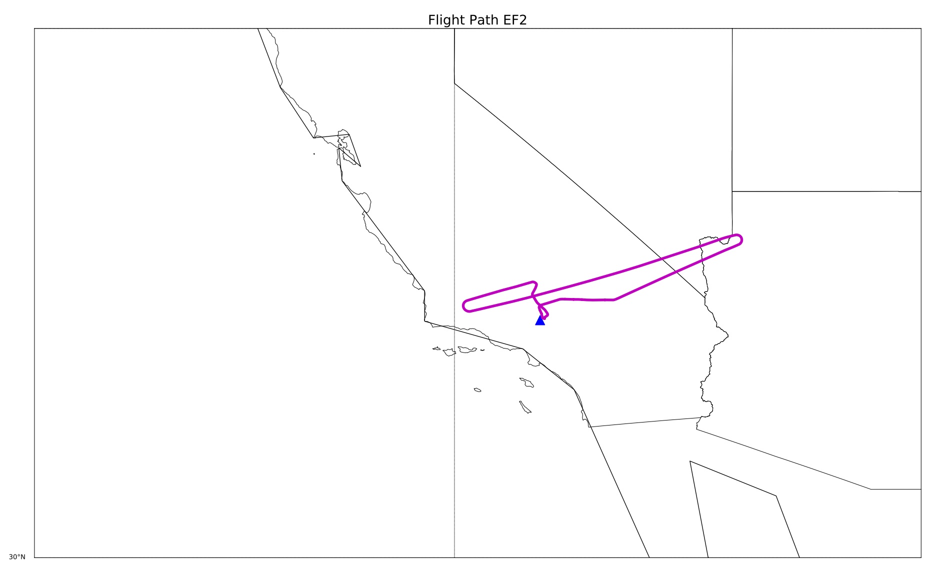

Figure 3. ER-2 flight path for engineering flight.

4.2 Aircraft Data

Figure 4 shows the temperature and altitude recorded by the ER-2 during the engineering flight. The aircraft reached a maximum altitude of 70,000 feet and maintained this height during the lunar tracking phase of the mission. At 70,000 feet, the aircraft maintained its tracking heading for a duration of forty minutes, at which point the system was actively tracking the Moon within an ambient temperature of $-55^{\circ} C$.

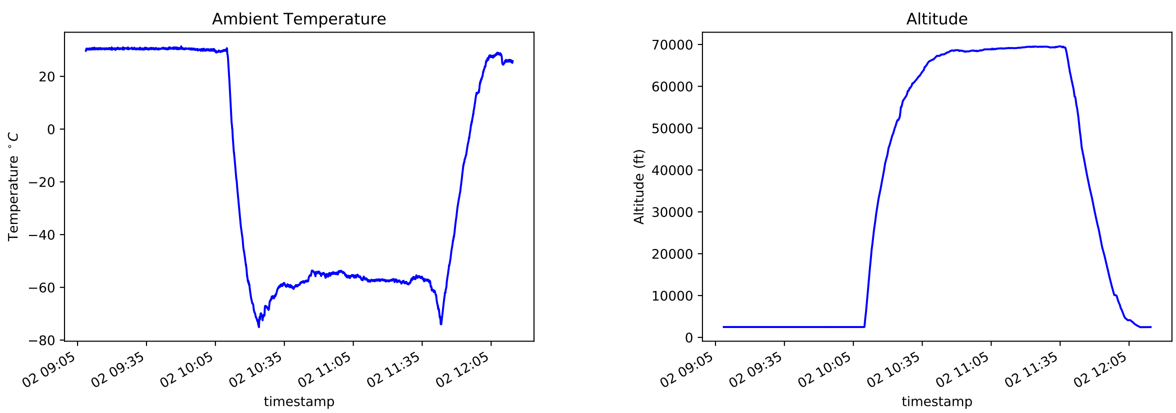

Figure 4. ER-2 temperature and altitude data

4.3 Tracking Performance

The performance of the robotic subsystem that was responsible for managing the pointing and lunar tracking of the telescope was evaluated by recording the radial pixel separation between the Moon and the setpoint within the image frames of the tracking camera. The radial pixel distance was calculated by adding the x and y pixel offsets in quadrature. Overall, the robotic system managed to track the Moon with a Root Mean Squared Error (RMSE) of 1.12 pixels. Using a conversion factor the pixel error corresponds to an RMSE traking error of 0.059 degrees over the tracking phase of the mission. Figure 5 shows a times series of radial offset pixel measurements over the course of the forty minute tracking window while table 1 outlines some of the more meaningful tracking statistics used to evaluate the systems overall tracking performance, and the performance of the two independent controllers responsible for adjust the telescope's pointing in azimuth and elevation.

The bar chart represented by Figure 6 provides a concise summary of the performance of the system's performance in azimuth and elevation. The y axis of the chart is the percentage of data points that fall within a given error while the x axis represents a pixel error separating the target from the setpoint in x and y. By refering to the chart, we can observe that of the total data points collected during the mission, over 90% placed the Moon within ± 1 pixel of the setpoint in both x and y. From Figure 6 we can also deduce that the tracking performance of the elevation controller was slightly worse when compared to the azimuth. This could be a result of having less optimal gain settings for the elevation controller or that the system is subjected to greater disturbances in elevation than in azimuth.

Statistic	X	Y	Radial Offset	Degree Offset
Min. Val.	-5.00	-5.00	0.00	0.000°
Max. Val.	6.00	4.00	6.32	0.335°
RMSE	0.74	0.84	1.12	0.059°

Table 1. Tracking statistics for pixel error

4.4 Raw Uncalibrated Lunar Spectrum

Due to proprietary concerns, only the raw uncalibrated spectrum could be included. The following figure shows the first lunar spectrum captured from an altitude of 70,000 feet. The spectrum was a result of over 270 spectral

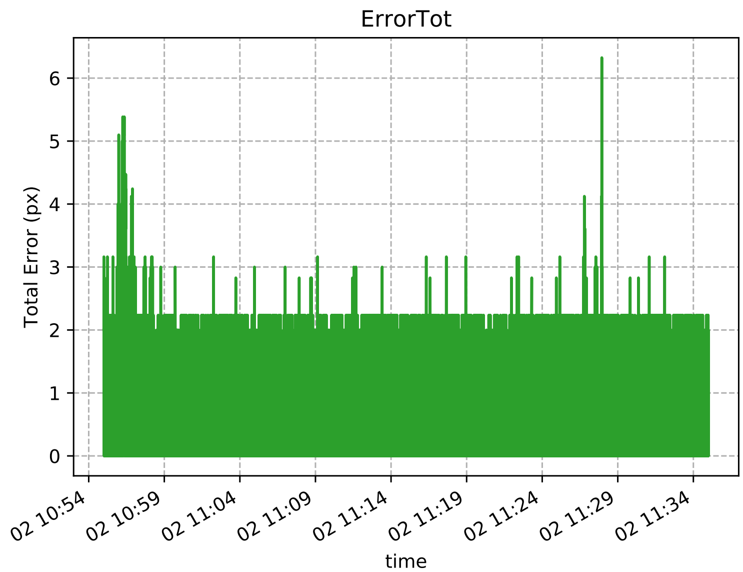

Figure 5. ARTEMIS tracking performance.

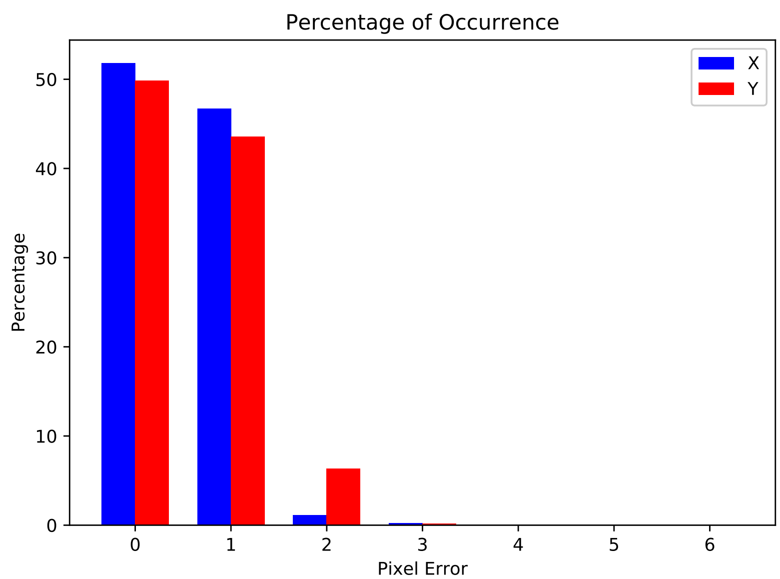

Figure 6. ARTEMIS tracking performance in x and y image coordinates.

scans of the Moon taken over the 40 minute tracking window. The spectral measurements were remarkably consistent and showed very little variance. As expected, by flying above the Earth's atmosphere, no lunar wavelengths were lost or obstructed. Had this spectrum been captured from the ground, it would have shown large valleys for shorter wavelengths where no light intensity or counts were measured. This spectrum however shows exceptional completeness for all wavelengths which is impossible to capture from ground based systems due to the obstruction of key lunar wavelengths from the Earth's atmosphere.

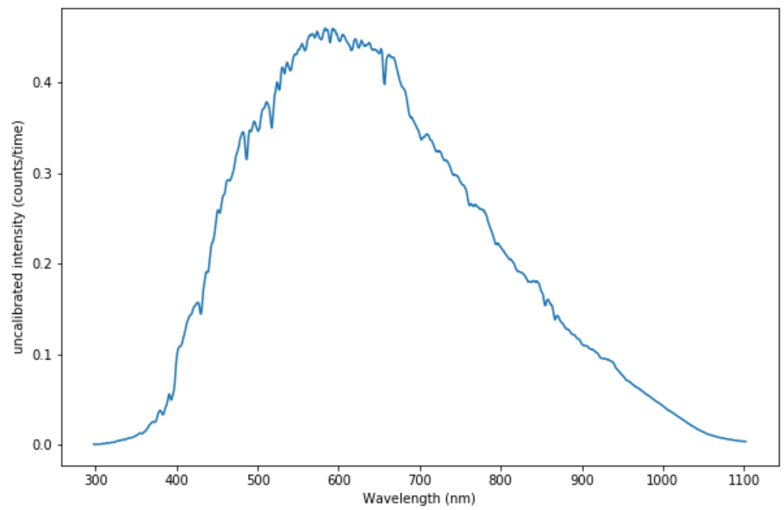

Figure 7. Raw uncalibrated lunar spectrum.

5. CONCLUSIONS

In conclusion, the first deployment of the air-LUSI project was an extraordinary success. The simplified robotic strategy which uses linear actuators to manage the pointing and tracking of the telescope while in flight provide a robust and cost effective design that produced better than expected results. The system operated reliably in the high altitude environment for the entire 3 hour duration of the flight and allowed for over 270 lunar spectral scans to be acquired through out the 40 minute tracking window. The Lunar Spectrum that was acquired during air-LUSI's first set of engineering flights showed notable consistency and completeness. The spectrum shown by Figure 7 shows a complete spectrum for all wavelengths within the visible spectrum which is impossible to achieve from ground based measurement systems. Given the impressive results obtained from air-LUSI's first mission, Fall 2019 dates are being reviewed for a second set of science flights to target specific lunar phases. By acquiring a large High Altitude Lunar Spectral Irradiance dataset, air-LUSI may play a key role in refining a Lunar Calibration Model to meet its accuracy targets and improve the remote sensing capabilities of certain instruments in NASA's Earth Observing System.

ACKNOWLEDGMENTS

We would like to thank Steven Brown, Steven Grantham, Stephen Maxwell, Thomas Larason, and John Woodward at NIST for their extraordinary work in creating the IRIS subsystem of the air-LUSI instrument. A project of this size required significant collaboration and would not have been possible without their commitment and dedication. We also appreciate all of the assistance in integrating the robotic and radiometric designs of the air-LUSI instrument, and help with developing some of the control system software for the robotic system.

REFERENCES

[1] Miller, S. and Turner, R., "A dynamic lunar spectral irradiance data set for npoess/viirs day/night band nighttime environmental applications," *IEEE Transactions on Geoscience and Remote Sensing* **47**, 2316–2329 (July 2009).

[2] Xion, X., Sun, J., Fullbright, J., Wan, Z., and Butler, J., "Lunar calibration and performance for s-npp viirs reflective solar bands," *IEEE Transactions on Geoscience and Remote Sensing* **54**, 1052–1062 (February 2016).

[3] Barnes, R., Eplee, R., Patt, F., Kieffer, H., Stone, T., Meister, G., Butler, J., and McClain, C., "Comparison of seawifs measurements of the moon with the u.s. geological survey lunar model," *Journal of Applied Optics* **43**, 5838–5854 (November 2004).

[4] Eplee, R., Barnes, R., Patt, F., Meister, G., and McClain, C., "Seawifs lunar calibration methodology after six years on orbit," *Proceedings of SPIE Earth Observing Systems IX* **5542**, 1–13 (May 2014).

[5] Anderson, J., Becker, K., Kieffer, H., and Dodd, D. N., "Real-time control of the robotic lunar observatory telescope," *Publications of the Astronomical Society of the Pacific* **111**, 737–749 (June 1999).

[6] Stone, T. and Kieffer, H., "Use of the moon to support on-orbit sensor calibration for climate change measurements," *Proceedings of SPIE Earth Observing Systems XI* **6296**, 1–13 (August 2006).

[7] Zimmer, P., McGraw, J., Ackermann, M., Hines, D., Hull, A., Rossmann, L., Zirzow, D., Brown, S., Cramer, C., and Fraser, G., "Space-based photometric precision from ground-based telescopes," in [*Proceedings of SPIE Fround-based and Airborne Instrumentation for Astronomy III*], **7735** (2010).

[8] Osborne, J., Hicks, G., and Fuentes, R., "Global analysis of the double-gimbal mechanism," *IEEE Control Systems Magazine* **28**, 44–64 (September 2008).

[9] Masten, M., "Inertially stabilized platforms for optical imaging systems," *IEEE Control Systems Magazine* **28**, 47–64 (June 2008).

[10] Hurak, Z. and Rezac, M., "Image-based pointing and tracking for inertially stabilized airborne camera platform," *IEEE Transactions on Control Systems Technology* **20**, 1146–1159 (September 2012).

[11] Hurak, Z. and Rezac, M., "Combined line-of-sight inertial stabilization and visual tracking: application to an airborne camera platform," in [*Proceedings of the 48th IEEE Conference on Decision and Control and 28th Chinese Control Conference*], **1**, 8458–8463, IEEE, Publisher address (December 2009).

[12] Cook, B., Braun, D., Hankins, S., Keonig, J., and Moore, D., "Precision linear actuator for space interferometry mission (sim) siderostat pointing," in [*39th Aerospace Mechanisms Symposium*], (2008).

[13] B. Cook, e. a., "Precision linear actuator for space interferometry mission (sim) siderostat pointing," in [*Proceedings of the 39th Aerospace Mechanisms Symposium*], 8458–8463, Jet Propulsion Laboratory, Jet Propulsion Laboratory and National Aeronautics and Space Administration, Pasadena, CA (May 2008).

[14] R. Saulescu, e. a., "On the eccentricity effects in solar tracking triangular linkage with eccentric linear actuator," in [*Proceedings of the 39th Aerospace Mechanisms Symposium*], 8458–8463, IEEE, Publisher address (October 2007).

[15] Ultramotion Technical Staff, *Ultramotion Servocylinder Information and User Manual Version*. Ultramotion Inc, Cutchogue, New York, a.07 ed. (2017).

[16] Wang, H. and Williams, T., "Strategic inertial navigation systems," *IEEE Control Systems Magazine* **28**, 65–85 (February 2008).

[17] Kamatics RWG Technical Staff, *KAron Design Guide*. Kaman Specialty Bearings and Engineered Products, Bloomfield, Conneticut, n.a. ed. (2012).

[18] Kamatics RWG Technical Staff, *KAron Bearing Catalog: Spherical, Rod End, and Journal Sleeve Bearings*. Kaman Specialty Bearings and Engineered Products, Bloomfield, Conneticut, n.a. ed. (2013).

[19] Park, J., Bahn, L., hun Lee, C., il Kim, T., soo Kim, K., and il Cho, D., "A novel method for vision tracking with line of sight control using a fuzzy logic controller and euler angle orientation in the feedforward loop," in [*IEEE 8th International Conference on Ubiquitous Robots and Ambient Intelligence (URAI)*], (2011).

[20] Baek, I., Gadsden, S. A., Cho, B.-K., Lee, H., and Kim, M., "Whole-surface round object imaging method using line-scan hyperspectral imaging system," in [*Proceedings of SPIE Sensing for Agriculture and Food Quality and Safety VIII*], *Commercial + Scientific Sensing and Imaging* **9864**, 8458–8463, SPIE (May 2016).

[21] Chittle, J., Biglarbegian, M., and Gadsden, S. A., "Mobile robot tracking using an overhead camera and sensor fusion," in [*2018 IEEE Canadian Conference on Electrical and Computer Engineering (CCECE)*], (2018).

[22] Okamoto, J. and Grassi, V., "Visual servo control of a mobile robot using omnidirectional vision," in [*Proceedings of Mechatronics*], 413–422, University of Twente (June 2002).

[23] Park, J., Hwang, W., Kwon, H., and Kim, K., "A novel line of sight control system for a robot vision tracking system, using vision feedback and motion-distrubance feedforward compensation," *Robtica* **31**, 99–112 (January 2013).

[24] Shiao, Y.-S., "Design and implementation of real-time tracking system based on vision servo control," *Tamkang Journal of Science and Engineering* **4**(1), 45–58 (2001).

[25] Kim, J., Chang, K., Schwarz, B., Lee, A., Gadsden, S. A., and Al-Shabi, M., "Dynamic model and motion control of a robotic manipulator," *Atlantis Press Journal of Robotics, Networking and Artificial Life* **4**, 138–141 (July 2017).

[26] Gadsden, S. A., "An adaptive pid controller based on bayesian theory," in [*ASME Dynamic Systems and Control Conference*], (2017).

[27] Bonadies, S., Smith, N., Niewoehner, N., Lee, A., Lefcourt, A., and Gadsden, S. A., "An overview of autonomous crop row navigation strategies for unmanned ground vehicles," *ASME Journal of Dynamic Systems, Measurement, and Control* **140**, 1–6 (September 2017).

[28] Attari, M., Habibi, S., and Gadsden, S. A., "Target tracking formulation of the svsf with data association techniques," *IEEE Transactions on Aerospace and Electronic Systems* **53**, 12–25 (February 2017).